Effect of Urbanization on Tree Growth in Remnant Forest Patches

By Teegan McClung

A thesis submitted
in partial fulfillment of the requirements
for the degree of
Master of Science
(Natural Resources and Environment)
at the University of Michigan
March 2017

Faculty advisor(s):
Ines Ibáñez, Associate Professor
Bob Grese, Professor

Abstract:

Land conversion and increasing impervious surface cover are affecting forests across the landscape by increasing local temperatures and altering ecosystem processes. In this study, we assessed the impact of impervious surface cover and other environmental, landscape, or climate factors on the growth of trees in adjacent forest patches. Tree cores were collected from 36 *Acer saccharum*, 40 *Carya ovata*, and 45 *Quercus rubra* trees in 11 deciduous forests in Southeastern Michigan and their annual radial growth measured from 1985 to 2014. Soil and stand basal area data were collected in each forest and distance from edge, mean impervious surface percentage within 250 m, and percent slope were calculated for each individual from National Land Cover Datasets. Annual average temperature, total precipitation, and Palmer Drought Severity Index data was also collected from the National Climatic Data Center.

Tree growth rate was modeled by species and diameter using a Bayesian framework with non-informative priors as a function of percent impervious surface. Running models with several combinations of explanatory variables (distance to edge, slope, percent sand, total nitrogen, basal area, and climatic variables) did not improve the goodness of fit so random effects terms for individual growth and year were added, in addition to antecedent terms, which helped account for the potential effect of previous years' growth.

The model resulted in R^2 values of 0.67 for *A. saccharum,* 0.71 for *C. ovata*, and 0.88 for *Q. rubra*. Higher levels of impervious surface did significantly, negatively affect the growth of small *A. saccharum* individuals and growth in an individual is strongly dependent of growth from the previous year. The year random effects term showed weak correlations with summer temperatures (-), spring and summer (+) precipitation, and the Palmer Drought Severity Index (-). These observations imply that not all trees species and size classes are affected equally by urbanization. Remnant forest patches typically experience little to no management and largely need to be self-sustaining over time, which highlights the need for a better understanding of how urbanization will affect these ecosystems.

Acknowledgements:

I would like to sincerely thank my adviser, Inés Ibáñez, for her ongoing faith in me and support of this project. I am so honored to have worked with you and learned so much for your experience. I would like to thank my committee member, Bob Grese, for welcoming me to SNRE when I first arrived and remaining a positive, knowledgeable, helpful presence throughout my time in the program. I would also like to thank the Global Change Ecology Lab for their help, both in the field and the office, especially Julie McLaughlin, Caleb Fogel, Natalie Tonn, Dan Katz, Elan Marguiles, Ben Lee, and Ben Conor-Barrie. Last but not least, I would like to thank my friends and family for their invaluable emotional support and my husband, Dan McClung, for his enduring belief in me and ceaseless ability to encourage me when I was stuck.

This work was financially supported by the School of Natural Resources and the USDA National Institute of Food and Agriculture, (McIntire Stennis project 1003470 to T.M. and I.I. And to I.I. by NSF DEB 1252664) and would not have been possible without the University of Michigan and the City of Ann Arbor, who allowed me access to the forests and natural areas, in which I collected my data.

Table of Contents:

List of Tables:

List of Figures:

Introduction

Anthropogenic drivers of global change, i.e., land-use alteration, introduction of new species, pollution and changing climatic regimes, are affecting forest composition and function across the landscape (Coomes et al. 2014). In particular, landscape changes and their effects on remnant vegetation constitute one of the major stressors on natural ecosystems (Sala et al. 2000). In the case of forests, up to 70% of remaining forested area around the globe is less than 1 km from the forest's edge (Haddad et al. 2015). As land is urbanized, the effects of the conversion on the remaining vegetation become more apparent. By increasing local temperatures and altering hydrologic and nutrient cycling, land conversion and increasing impervious surface cover has been found to affect forest health and forest resilience to other stressors (Gavier-Pizarro et al. 2010, Kaye et al. 2005, Matlack 1993, McDonnell et al. 1997). Still, these remnant patches of natural forest are critical to improving air quality, reducing flooding, tempering the urban heat island effect and providing other ecosystem services that are important to both human societies and nature as a whole (Xiao et al. 1998, Nowak et al. 2006). Therefore, understanding how urbanization affects the health of tree species in remnant forest patches becomes critical to both conservation and management of this resource.

One of the primary changes that accompanies urbanization is the increase in the amount of land covered by impervious surfaces such as pavement, buildings, and highly compacted soils. Percent impervious surface is a reliable predictor of changes in land surface temperature and an appropriate proxy for urban heat island effects (Yuan and Bauer 2007, Zhou et al. 2014). Urban heat islands develop around areas with low albedo and high absorptive capacity such as asphalt, bare-soil, and other developed surfaces, which heat up rapidly and can increase localized temperatures by as much as 10 ºC over temperatures in adjacent woodlands (Kim 1992). In a 2015 study by Jiang et al., land converted from forest cover to commercial cover experienced a more than 70% increase in land surface temperature and a 15% decrease in soil moisture. These changes in the microclimate of urbanized areas can affect the remnant vegetation. One small-scale study found a trend of lower drought resilience but higher growth rates in trees growing in high-impervious covered areas when compared with trees in forested areas (Fahey et al. 2013). In another study, Cregg and Dix (2001) found that trees in urban environments experience greater moisture stress and

insect damage when compared with trees in intact forests. In general, increasing impervious cover correlates with increasing water stress and vulnerability to drought, having trees in more urbanized landscapes higher vulnerability to cavitation and lower protection from embolism formation (Savi et al. 2015).

The impact of these land-use changes on tree health can be estimated by measuring changes in annual tree growth. Trees radial growth is a good indicator of the tree's health status. Trees with lower rates of growth have been found to have higher rates of mortality over time (Wyckoff and Clark 2002). Radial growth can be affected by the frequency of precipitation, with diffuse porous species, such as *Acer spp*., being more sensitive than ring porous species, such *Quercus spp.*, to more variable precipitation (Elliott et al. 2015), and by maximum temperatures (Martin-Benito and Pederson 2015). Also, the seasonal timing of climatic events such as drought can have differential effects on radial growth, with spring drought exhibiting a greater influence on radial growth than drought at other times of the growing season (Foster et al. 2014). Further, *Quercus spp.* have been found to have more growth variability in drier warmer sites than in wetter cooler areas (White et al. 2010).

Trees experience a shorter time to mortality when drought conditions are accompanied by a temperature increase of approximately 4º C, which is likely a result of internal carbon starvation from elevated respiration rates in conjunction with lower photosynthetic rates in response to stomatal closure (Adams et al. 2009). Therefore, increasing urbanization could compound the impact of climate change on trees. Increases in temperature are to be accompanied by more severe and frequent droughts that could increase tree mortality (Winkler et al. 2012, Gustafson and Sturtevant 2013). Even if most forest species are able to tolerate changes in mean climatic conditions it is not clear that they will be able to withstand the effects of extreme weather events like drought (Suarez et al. 2004, Pasho et al. 2011). Thus, the synergistic effects of detrimental weather events, like drought, and the increase in temperature associated with urban areas could have a strong impact on the health and resilience of trees growing in urban settings. A decline in forest health and a change in species composition would alter environmental services and ecosystem processes in these ecosystems. Remnant forest patches typically experience little to no management and largely need to be self-sustaining over time, which highlights the need for a better understanding of how urbanization will affect these ecosystems.

Most urbanization studies have focused on large cities, where the effects are likely to be most extreme, but most cities around the world are small or medium size so it is important to understand how localized urbanization affects these prevalent areas. In this study, we investigated if tree growth rates were affected by the degree of urbanization surrounding remnant forest patches in a middle-sized city in Southeastern Michigan, USA. In particular, we assessed how the percent of impervious surface affected the growth of *Acer saccharum*, *Carya ovata*, and *Quercus rubra* in remaining vegetation patches along an urban to rural gradient. We hypothesized that an increase in impervious surface would decrease annual tree growth in all trees, but most significantly in *A. saccharum*, a highly drought intolerant species, due to a decrease in ground water availability and an increase in localized temperatures. We developed an individual based model to analyze the relationships between tree growth and surrounding growth conditions. We then used this information to understand how growth rates might vary between these three native tree species along the urban gradient. The basic questions we address are: 1) Does impervious surface impact the growth of surrounding trees and does this impact change based on species or tree size? 2) Which other environmental factors may also play a role determining tree growth in urban areas? 3) Do temperature and precipitation changes differentially affect tree growth depending on the surrounding percentage of impervious cover? Understanding the *in situ* responses of the current forest communities to the changing environmental conditions, will be critical to forecast the response of remnant forests to urbanization.

Methods

Study sites

This study was carried out in Southeastern Michigan along a twenty-mile urban-rural gradient from the city of Ann Arbor, Michigan (population: 113,934; US Census Bureau 2010) to Pinckney State Recreation Area, northwest from the city (Fig. 1). We collected samples from 11 deciduous forests, with surrounding impervious cover ranging from 0 to 35 percent (Table 1, Fig. 1). These forests were typically logged more than once prior to 1940 and some were used for agriculture or grazing before reforestation was allowed to occur. Bird Hills Natural Area, Edwin S. George Reserve, Saginaw Forest, and Stinchfield Woods all have areas that were planted with conifer species with patches of natural deciduous forest.

Berkshire Creek, Stapp Nature Area, and Scarlett Mitchell Nature Area were purchased by the city of Ann Arbor in the early 2000s to save the properties from development. Nichols Arboretum and Horner McLaughlin Woods were donated to the University of Michigan to serve as botanical sanctuaries and displays. Sites were selected based on access-consent and the presence of multiple individuals of at least two of the following species: *Acer saccharum, Carya ovata*, and *Quercus rubra.* We established one sampling location in each of the smaller forest fragments, Berkshire Creek Nature Area, Stapp Nature Area, Saginaw Forest, Radrick Forest, an unnamed area on the UM North Campus, Edwin S. George Reserve, and Stinchfield Woods. In the larger forests with surrounding urban development, Bird Hills, Scarlett Mitchell, Horner McLaughlin and Nichols Arboretum, we established one or two sampling locations within 100 m of the forest edge and one location greater than 200 m from the forest edge, for a total of 16 locations in 11 forests (Table 1).

Study species and tree cores

We chose to analyze radial growth of *A. saccharum, C. ovata,* and *Q. rubra* because all three species are native, often found in the same stands, and common in the southern Michigan forests. They also represent a range of drought tolerances from intolerant (*A. saccharum*), to moderately tolerant (*Q. rubra*), to very tolerant (*C. ovata*; Abrams 1998, Cowden et al. 2014, Klos et al. 2009, LeBlanc and Terrell 2009), which allowed us to look at urbanization effects regardless of sensitivity to drought (Meinzer et al. 2013, Abrams et al. 1998, Tang et al. 2012). At each sampling location, we selected three trees to sample from each represented species with variable diameters (between 16.5 and 61 cm). For each selected tree, we recorded the diameter at breast height (DBH, 1.3 m) and Geographic Position System (GPS) coordinates, using a Garmin eTrex 10 GPS Device. One tree core was extracted from both the east and west sides of each tree using a 4.3 mm diameter Haglof increment borer. Sampling occurred between June and November of 2014.

In the lab, tree cores were dried, glued to pre-cut mounts, and then sanded. Samples were sanded using P150, P220, P320, P600, and P1200 (*A. saccharum* only). After sanding, cores were scanned using a Canon CanoScan LiDE 110 flatbed scanner with 1200 dpi resolution. The annual ring widths were then measured digitally using LignoVision by RINNTECH (vs. 1.37). East and west core measurements were averaged and then samples within each species

were cross-dated visually and using skeleton plots (Stokes and Smiley 1987). Cores that were broken or damaged were discarded. For each tree, we calculated the sum of the east and west cores (or the double of one side if the other was unusable) to estimate total diameter annual growth (mm) and then subtracted the annual growth iteratively from the current diameter to calculate the approximate DBH in each year. We focused on growth since 1985 (30 years) to reflect contemporary levels of urbanization.

Site data

To gather data about the land-use conditions surrounding each tree, we obtained four years of National Land Cover Datasets (NLCD; 1992, 2001, 2006, and 2011; Fry et al. 2011, Homer et al. 2007, Homer et al. 2015, Vogelmann et al. 2001), three years of impervious surface percentages (2001, 2006, and 2011; Xian et al. 2011), road alignments, and a Digital Elevation Model (DEM; MGDL 2014). The NLCD and DEM data shared 30 m resolution. In ArcGIS 10.2, we reclassified all of the landcover layers for each year of the NLCD into forest (including deciduous, evergreen, mixed, wetland sub-types) and non-forest and then calculated the distance from forest edge to each pixel (ESRI 2013). We used the zonal statistics tool in ArcGIS Spatial Analyst to calculate the mean impervious surface percentage within 250 m of each tree from the NLCD impervious surface maps and averaged the value across 2001, 2006, and 2011 maps to assign one representative value of impervious cover to each tree (ESRI 2013). We used percent impervious surface within a 250 m radius (*impervious*) as the proxy for the microclimatic effects due to urbanization. We used the DEM to calculate percent slope for each pixel.

We also collected tree basal area and soil samples from three places at each of the eleven sampling locations. At each site, we established three 10 x 10 m basal area plots that contained at least one of the sampled trees. In each plot, we recorded the DBH of all living trees greater than 3m tall and collected a combined total 100 g of soil from the top 10 cm for each sample. We converted the dbh into basal area and added all trees in the plot to determine total basal area for each plot and the results of all plots in a forest were averaged to determine the representative basal area value in cm^2/m^2. The soil samples from each location were sent to the Michigan State University Soil Laboratory for analysis of total nitrogen, pH, phosphorous, cations and percent sand, silt and clay, all variables known to affect tree growth

(e.g., Vicca et al. 2012, Levesque et al. 2016). The pH was measured using an electronic pH meter with a 1:1 water slurry. Cations and phosphate (PO_4^-) were extracted from 5-g sub samples with a Mehlich III solution. Concentrations of Mg^{2+}, Ca^{2+}, Cl^+, Na^+ and K^+ (ppm) in extracts were measured with Direct Current Plasma (DCP, SMI Corp., Glouchestershire, UK) atomic emission spectrometry, and the Alpkem Series 500 autoanalyzer was used to measure PO_4^- (ppm). Total N (mg/g) was measured using the Dumas method (Shea and Watts 1939). Particle size analysis (%) was done using the Bouyoucos Hydrometer method (Bouyoucos 1962).

We obtained data from the National Climatic Data Center, Southeast Michigan (Region 10) from 1985 to present monthly average temperatures, total precipitation and Palmer Drought Severity Index (PDSI; NCDC 2015).

Data analysis

We developed a model to examine the influence of surrounding landscape conditions on annual tree growth from 1985 to 2014. Here we assume that the level of land development has been constant during this period of time, land cover data were relatively unchanged during the period of time we have access to, 1992 to 2011. To address the well-established, size-dependent relationship between tree size, or age, and growth rate, with higher growth at smaller diameters (or younger cohorts; Mérian and Lebourgeois 2011), we divided the data, and analyzed accordingly, into three diameter classes, small (<25 cm), medium (25-40 cm), and large (>40 cm). Only small and medium size classes were analyzed for *A. saccharum* as the maximum dbh recorded was 45 cm. We then ran several models with several combinations of explanatory variables, e.g., distance to edge, slope, percent sand, total nitrogen, basal area, and climatic variables, but these variables did not improve the fit of the model (based on goodness of fit). We describe below the model that best predicted the data (higher R^2 predicted *vs* observed). Each species was analyzed independently.

We analyzed growth rate as a function of percent impervious surface within a 250 m radius (*impervious*) of each tree as the proxy for urbanization with β as an intercept. The model included an intercept (α). To account for the potential effects that previous years' growth could have on current year growth (Peltier et al. 2016), we also included antecedent effects (Ogle et al. 2015). Antecedent effects of previous growth (*PG*) were estimated as a

function of growth (G) during the previous three years: $PG_t = \omega_1 G_{t-1} + \omega_2 G_{t-2} + \omega_3 G_{t-3}$with λ as the intercept. Where ω are the weights given to each year ($\sum_{k=1}^{3} \omega_k = 1$). We also added an individual random effect term (*IRE)* to represent the individual growth variations that we could not account for with our data (e.g., genetic differences, competitive ability, neighborhood processes, access to nutrients). We considered climatic variables, i.e., temperature, precipitation, and drought index data in the model, but we were not able to achieve good convergence so we decided to include a year random effect term (*YRE*) to represent inter-annual variation in growth across all trees. We then calculated Pearson's correlation values between these YREs and average monthly temperature, precipitation and Palmer Drought Severity Index to further explore the influence of climate on growth for each species.

Growth for tree *i* in year *t* ($G_{i,t}$) was modeled with a normal likelihood (limited to be positive, a log-normal model was difficult to run)

$$G_{i,t} \sim Normal\left(Gm_{i,t}, \sigma^2\right)$$

and process model:

$$Gm_{i,t} = \alpha + \lambda \cdot PG_{i,t} + \beta \cdot impervious_{site(i)} + IRE_i + YRE_t$$

Parameters α, λ, β, and parameters ω for the calculation of *PG*, were estimated for each diameter class (small, medium and large). Given the inclusion of random effects and of antecedent effects, parameters were estimated using a Bayesian framework (Clark 2005). Parameters prior distributions were not informative, α, λ, β~*Normal*(0,10000), IRE, YRE~*Normal*(0,σ_*^2), σ_*~*Uniform*(0,100), and ω_*~*Dirichlet*(1/3,1/3,1/3). Analyses were run in OpenBugs ver 3.2.3 (Lunn et al. 2009, see supplement for code). We concurrently ran three Markov Chain Monte Carlo simulations for 300,000 iterations. After chains converged, we estimated posterior parameter means, 95% credible intervals, and standard deviations. We then used parameter means, variances and covariances to simulate growth under a gradient of impervious surface values.

Results

We sampled a total of 121 trees with 36 *A. saccharum* individuals at 9 sites, 40 *C. ovata* individuals at 10 sites (one core pair unusable), and 45 *Q. rubra* individuals at 11 sites (two core pairs unusable). Tree diameters for *A. saccharum* ranged between 13.1 and 45.2 cm,

with an average of 27.28 cm; *C. ovata* ranged between 21.6 and 58 cm, average 35.93 cm; and *Q. rubra* range from 16.5 to 61 cm, averaging 36.63 cm. Sampling in the 11 forests with 16 sites covered a wide range of landscape variation (Table 1, Supplemental Information). Impervious surface ranged from 0 to 35.08 %. Distance from edge ranged from 0 to 218.4 meters. Slope ranged from 0 to 106.7 % (with 45 degrees equaling 100 %). Model fit (goodness of fit R^2, predicted *versus* observed data) was 0.67 for *A. saccharum*, 0.71 for *C. ovata*, and 0.88 for *Q. rubra* (Supplemental Information).

Effects of impervious surface on tree growth - The level of impervious surface surrounding trees had no effect on the growth of *C. ovata* and *Q. rubra* individuals of any size category (β parameters, 95%CI overlapped with zero). It had a negative and significant effect on small diameter *A. saccharum* trees, and a negative, but not statistical significant effect on medium size *A. saccharum* trees (Fig. 2; Supplemental Information).

Effects of previous years' growth on current year growth - Annual growth was significantly, positively affected by growth in the previous years for all species and size classes except in small *C. ovata* trees (λ parameters; Fig. 3). Growth during one year prior had the largest effect on growth in the current year, with parameter estimates for the antecedent effects in the previous year (ω_1 parameters) ranging from 0.69 in small *A. saccharum* to 0.94 in large *Q. rubra* (Supplemental Information).

Year random effects - YRE, estimated for all trees of each species, were weakly and negatively correlated with average monthly temperatures from June through August of the current year, and positively correlated with May temperature in both *C. ovata* and *Q. rubra*. Precipitation was weakly, positively correlated with YRE for *A. saccharum* in June and August, *C. ovata* from May through September, and *Q. rubra* from June through August. Correlations between YRE and the Palmer Drought Severity Index were unexpectedly negative, which would indicate higher growth with higher drought (more negative values on the PDSI), except for *C. ovata* in August and September (Table 2; Fig. 5).

Growth simulations - In general growth simulations show the large range of variability found in the data (Fig. 4) and illustrate the higher growth rates in small *A. saccharum* trees at lower levels of impervious cover than at higher cover (Fig. 4). The growth of medium *A.*

saccharum and all size classes of *C. ovata* and *Q. rubra* was unaffected by increasing impervious surface cover.

Discussion

The global trend of increasing urbanization is generating isolated patches of vegetation that could be strongly influenced by the surrounding landscape. How these changes in landscape cover impact remnant forest patches are not well understood, and these impacts could cause shifts in forest health and forest resilience to other stressors. In this study, we aimed to determine if the percent of adjacent land covered by impervious surface, our proxy for the heat island effect and reduced soil moisture associated with urbanization, impacts the growth of trees in remnant patches and if this impact is species or size dependent. Further, we were interested in determining which other factors might interact with urbanization in their effects to tree growth, in particular we were interested in assessing if climatic events, i.e., drought conditions, may differentially affect tree growth depending on the surrounding percentage of impervious cover. We found that higher levels of impervious surface did affect the growth of small *A. saccharum* individuals, and these effects were negative. We also found that growth in an individual is strongly dependent of growth from the previous year. These observations imply that not all trees species and size classes are affected equally by urbanization and that individual growth characteristics could dominate growth patterns.

Although we found that the level of impervious surface surrounding trees had no effect on the growth of *C. ovata* and *Q. rubra* individuals of any size category, it did have a negative impact on *A. saccharum*. Impervious surfaces have been shown to increase local temperatures and alter local hydrological regimes, locally simulating drought conditions (Albrecht 1974, Kim 1992, Shuster et al. 2005). *A. saccharum* is the most drought intolerant species in our study, and a resulting negative growth response to increasing impervious surface would exemplify a possible amplification of localized drought conditions. We may not have seen a response in *C. ovata* or *Q. rubra* due to their higher drought tolerance or potentially because they are an older population of trees, in which drought intolerant individuals have already died in previous drought events (average dbh was higher for these two species).

Total annual growth of trees in a forest increases with proximity to the forest edge (McDonald and Urban 2004, Reinmman and Hutyra 2016). In our alternative models we did not see a response to proximity to edge, so we did not include this variable in the final model. This lack of response in our data may be due to the fact that edge trees are also more negatively impacted by high temperatures, indicating potential complex interactions between increased light availability and decreased soil moisture.

We found growth within each individual tree was highly variable from year to year and this variability may be greater than any influence of adjacent land or environmental conditions. Annual growth was significantly affected by growth in the previous year for all species and size classes except in small *C. ovata* trees. Growth during one year prior had the largest effect on growth in the current year, with the lowest weight in small *A. saccharum* to highest in large *Q. rubra*. We saw a pattern of higher growth after years of high growth, a positive association. An ongoing pattern of higher growth from year to year may indicate that the individual is not impeded by competition and has enough access to nutrients to sustain higher rates of growth (Gomez-Aparico et al. 2011, Kunstler et al. 2010).

The year random effects, which we used to assess climatic influences, show weak correlations with temperature, precipitation and the Palmer Drought Severity Index overall. Generally, the weak negative correlation with summer temperatures indicate a potential negative effect under warming conditions likely due to a higher water demand caused by higher evapotranspiration rates. Unsurprisingly, precipitation was consistently positively correlated with all species for most of the growing season from April to September, indicating the importance of water availability for growth of these species. We found an unexpectedly negative correlation between YRE and the Palmer Drought Severity Index. Typically, larger trees are more sensitive to summer drought than smaller trees (Mérian and Lebourgeois 2011) but we did not see a strong relationship between diameter growth and the summer Palmer Drought Severity Indices in our study. Our study was limited by sample size and coarse spatial resolution of both landscape and climate variables. Tree sampling design can influence variability and uncertainties in tree-ring studies (Nehrbass-Ahles et al. 2014). We used data with 30 m resolution for several environmental variables, including slope and distance to forest edge. Having a finer spatial scale these variables would have aided to explain some of the variability in data. Similarly, we used regional climate data rather than

spatially extrapolated climate data so we had to rely on impervious cover to approximate any urban hear island effects in the Ann Arbor area.

Understanding the ecological resilience, i.e., the on-going capacity of a forest to persist and recover after disturbance, to changing environmental conditions, and maintain overall ecosystem structure and function (Walker et al. 2004, Churchill et al. 2013), becomes essential to assess the potential effects of global change on forest ecosystems. In this study, we found that three of the common tree species are relatively resistant to the potential impact of urbanization and increasing impervious cover. Although, smaller *Acer* individuals could be less resilient to change over time and this could lead to a change in the composition of remaining urban forest patches. Although our study did not show strong relationships between climate and landscape factors, we cannot rule out the possibility of combined effects with accelerating land-use alternation and climate change. With the positive influence of precipitation, we also found that decreasing precipitation, such as drought events, could have a negative impact on some species in the urban forest as well, which could further alter the species composition of urban forests. Declines in forest health and subsequent changes in species composition could alter environmental services, like carbon storage, and other ecosystem processes provided by remaining forest patches, thus any impact on these forests should be considered when constructing predictive models and forest management plans.

Table 1. Forest sampling sites with geographic position, size, number of trees sampled in each location, percent impervious cover within a 250m radius, percent sand in soil samples, and soil pH. The site IDs correspond with Figure 1 and additional site information can be found in the Supplement.
**Edge and interior sampling locations, within 100 m of the edge and greater than 200 m from the edge*

Site Name	Site ID	Latitude	Longitude	Acres	ACSA	CAOV	QURU	% Impervious	% Sand	Soil pH
Nichols Arboretum*	1e,1i	-83.72883	42.40004	123	3	6	6	15.30±10.12	62.15±0.07	6.35±0.21
Berkshire Creek	2	-83.69823	42.25963	5		3	3	28.42±2.77	60	6.4
Bird Hills*	3e,3i	-83.75827	42.30719	153	6	3	6	0.93±0.64	61.25±8.84	5.75±0.21
Edwin S. George Reserve	4	-84.02105	42.45707	1300	3		3	0	83	5.3
Horner-McLaughlin*	5e1, 5e2, 5i	-83.66985	42.32228	90	9	9	6	3.31±3.88	42.73±7.36	5.73±0.32
North Campus	6	-83.70767	42.28486	35	3	1	3	3.11±0.35	73	6.4
Radrick Forest	7	-83.65731	42.28900	40	3	3	3	0.34±0.12	40	5.6
Saginaw Forest	8	-83.80473	42.27438	80	3	3	3	11.82±5.48	48.2	5.8
Scarlett Mitchell*	9e,9i	-83.69710	42.23390	25	3	6	6	9.38±6.92	55±7.07	5.7±0.57
Stapp	10	-83.71531	42.30844	8		3	3	24.43±1.40	49.5	6.4
Stinchfield Woods	11	-83.92737	42.39936	700	3	3	3	0	58.5	6.2

Figure 1. Forest sampling locations overlain on a landcover map created using the 2011 National Landcover Dataset (Homer et al. 2015), combing the landcover categories into Open Water, Developed Land, Forest, and Farm and Non-Forest Land (labels correspond to the Site ID provided in Table 1). The black lines show the boundaries of Washtenaw, Livingston, and Oakland Counties in Southeastern Michigan.

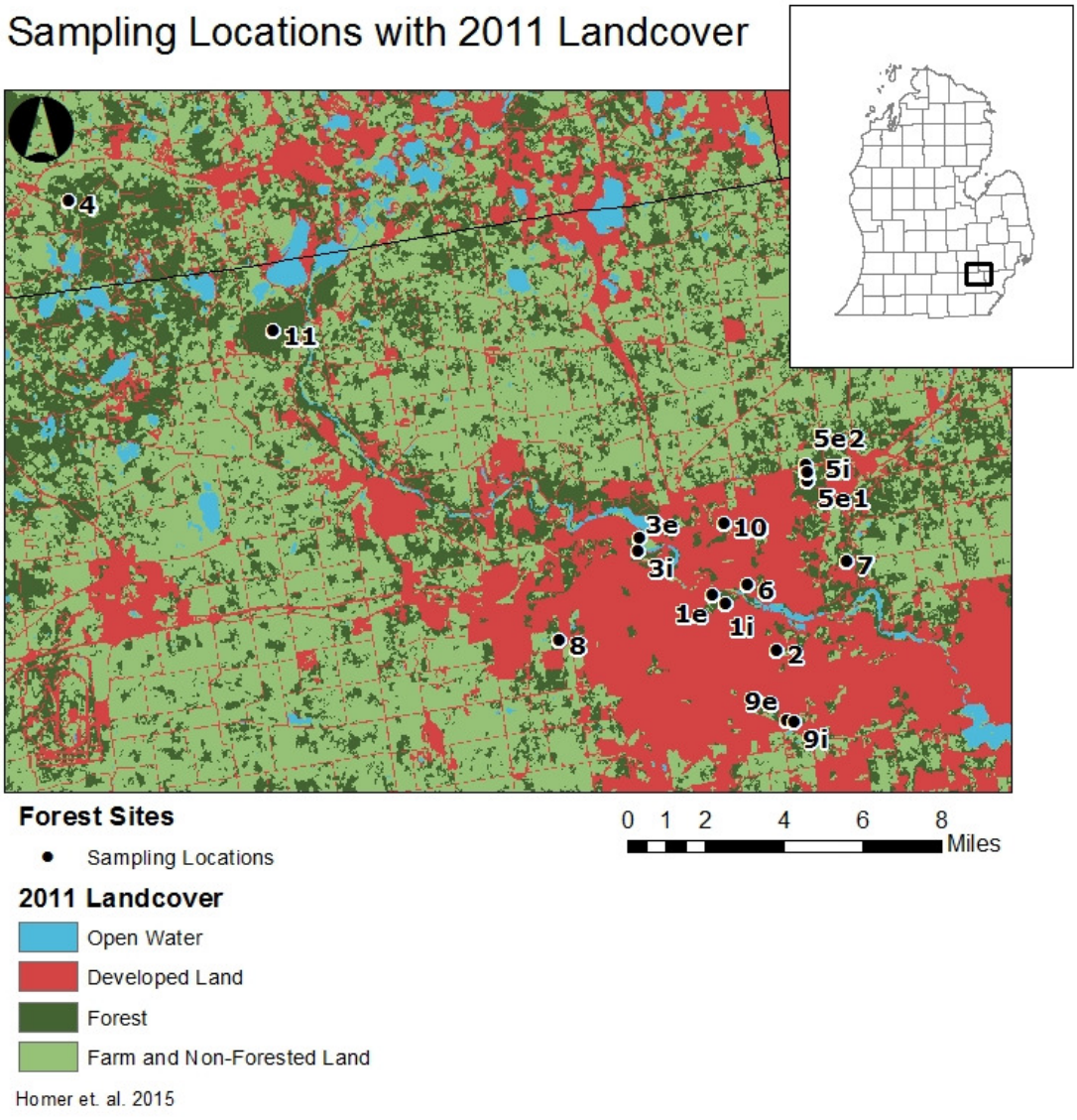

Figure 2. Parameter estimates for the impact of impervious surface on each species by size class. Each species is represented by a four letter abbreviation: ACSA – *Acer saccharum*, CAOV – *Carya ovata*, QURU – *Quercus rubra.* Growth of small diameter ACSA individuals was estimated to be significantly (*) negatively affected by increasing impervious surface cover. Growth of medium ACSA and all sizes of CAOV and QURU was not estimated to be significantly affected by impervious cover.

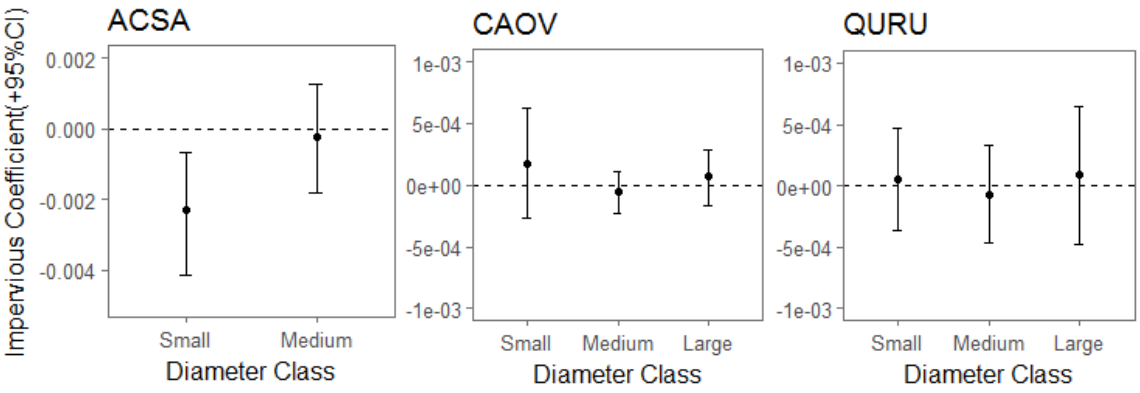

Figure 3. The relative weights of one (t-1), two(t-2), and three(t-3) year antecedent effects on tree growth by species and diameter class. The value of all three years must equal 1 so if all years equally contributed to predicting annual tree growth, we would expect all values to be 0.33 (dashed line). Values above 0.33 indicate a strong influence on annual growth, whereas values below 0.33 indicate a weak influence on annual growth. All values marked with an asterisk (*) are significantly different from 0.33.

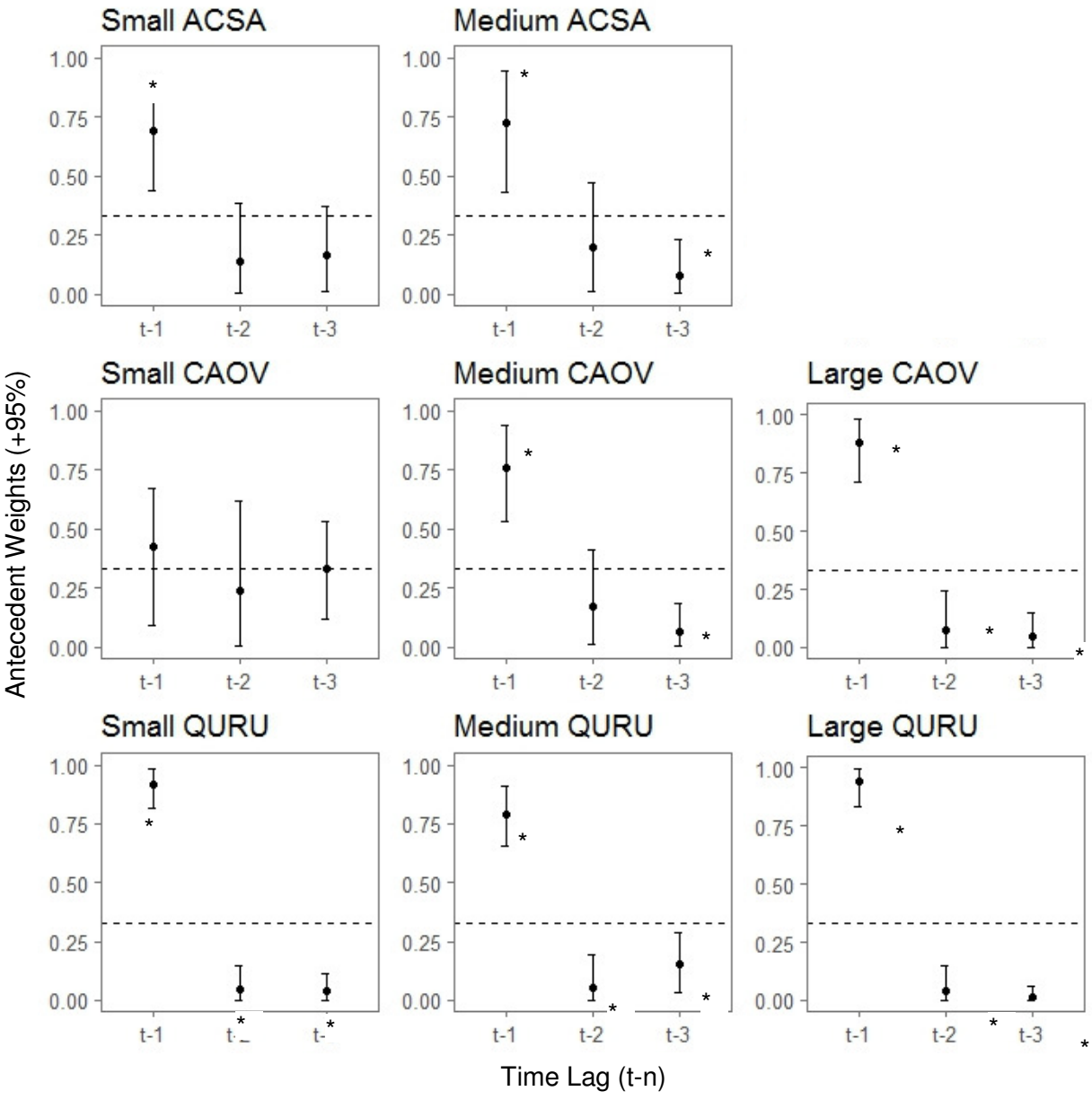

Figure 4. Growth predictions and measured growth for varying percentages of impervious surface cover. Solid lines show the prediction with 95%CI as a dashed line and dots show actual measurements from samples collected in the field by diameter class. Small ACSA shows a decrease in predicted growth with increasing impervious surface.

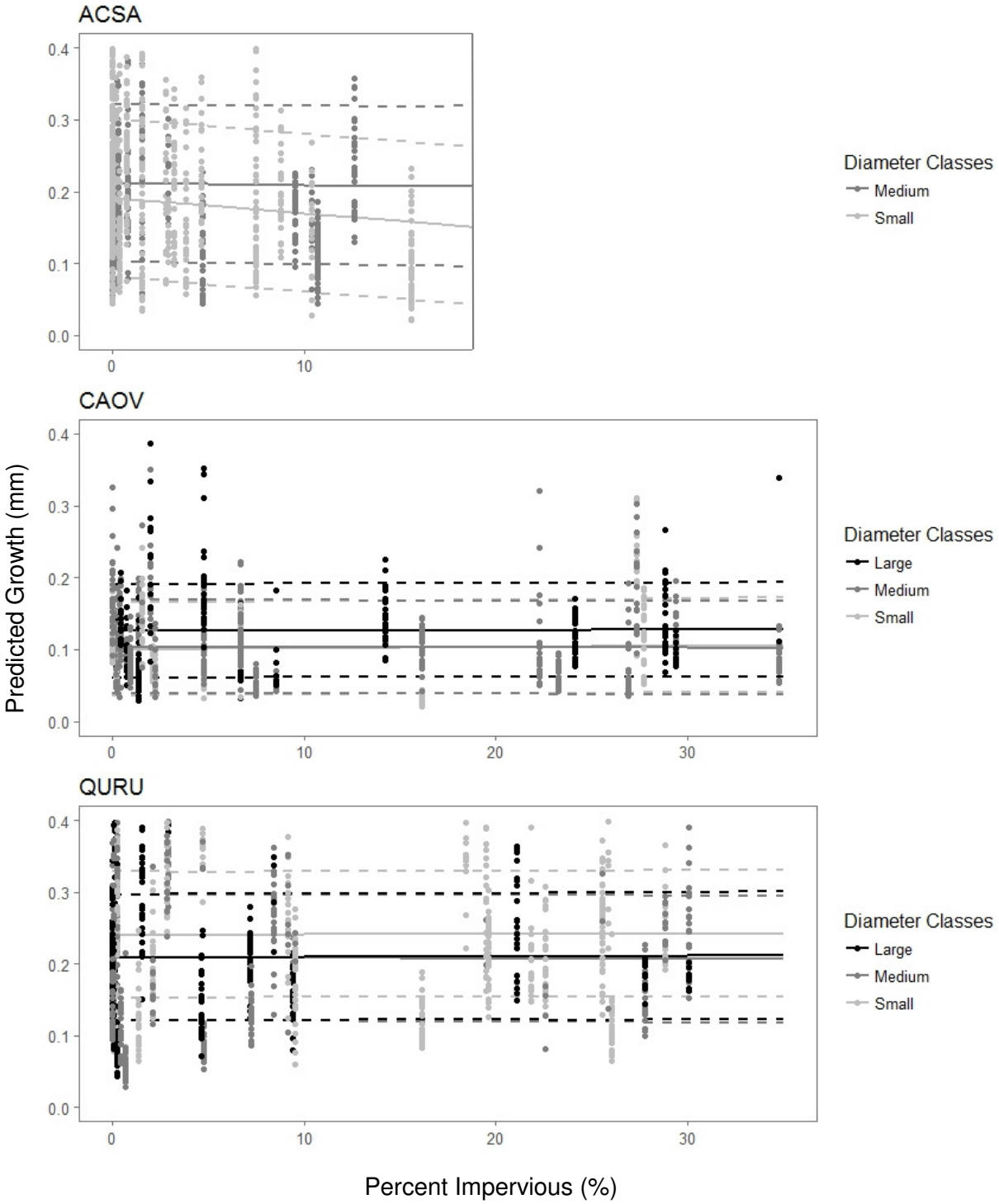

Figure 5. The model results for year random effects (YRE) by species, which was used to simulate climate in the model, is shown above graphs of average annual temperature, precipitation, and Palmer Drought Severity Index values from June through August of each year.

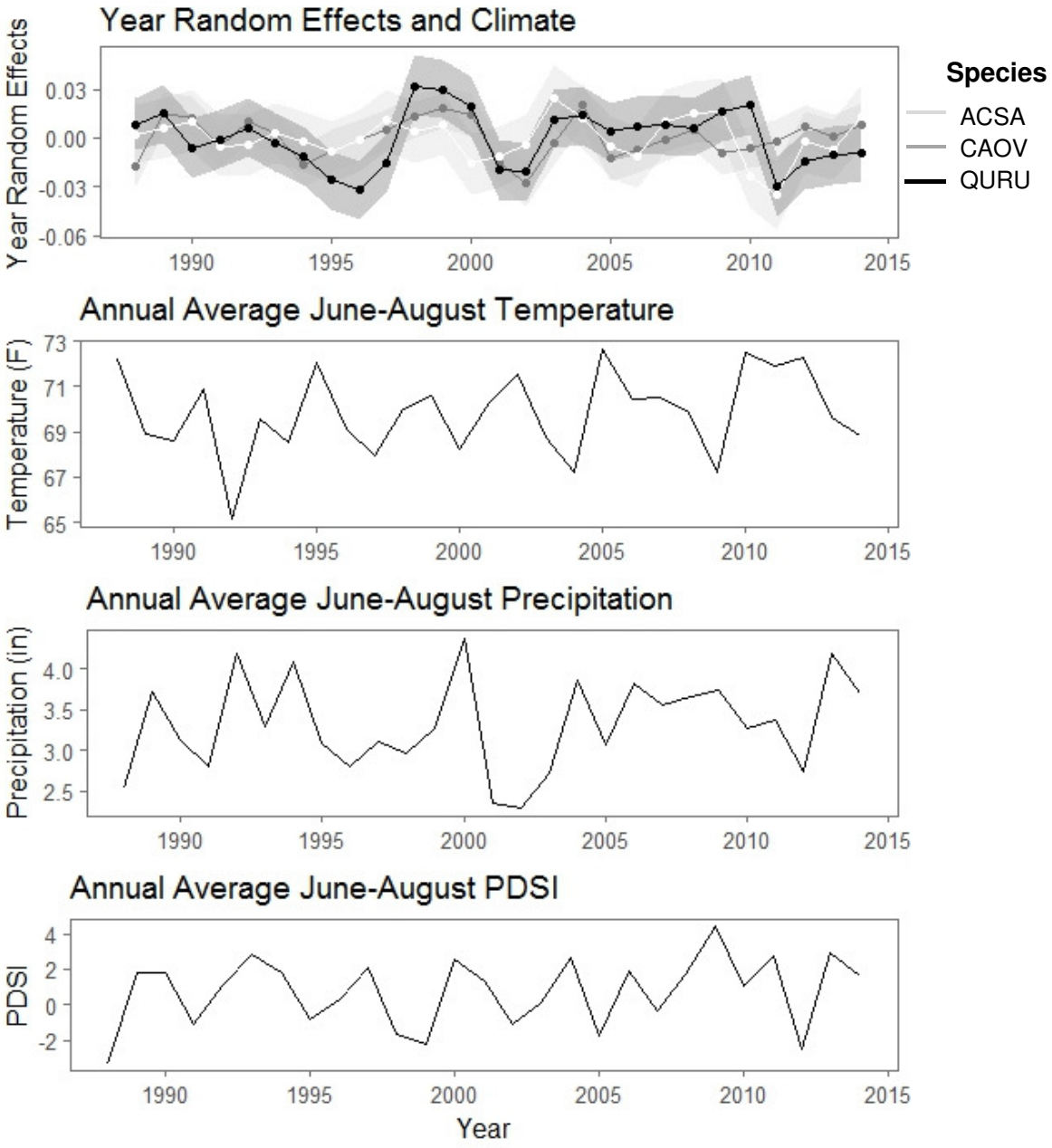

Table 2. The Pearson's correlation coefficients for YRE and climate variables show that climate in the current year correlates more with the year random effects than climate from the previous year. We also found a generally negative correlation with temperature (higher temperatures result in lower annual growth), a positive correlation with precipitation ((higher precipitation results in higher annual growth), and a negative correlation with PDSI (higher PDSI indicates wetter conditions and our results indicate lower growth with wetter conditions).

	Previous Year						Current Year					
Average Temperature	Apr	May	Jun	Jul	Aug	Sep	Apr	May	Jun	Jul	Aug	Sep
ACSA	-0.36	-0.26	-0.11	-0.03	0.00	0.09	-0.08	-0.29	-0.30	-0.46	-0.31	0.16
CAOV	-0.31	0.02	-0.03	0.11	0.00	0.09	-0.17	0.20	-0.32	-0.28	-0.51	-0.11
QURU	0.15	-0.10	-0.05	-0.07	-0.24	0.40	0.39	0.35	-0.18	-0.14	-0.14	0.25
Average Precipitation	Apr	May	Jun	Jul	Aug	Sep	Apr	May	Jun	Jul	Aug	Sep
ACSA	-0.07	-0.16	-0.14	-0.16	0.12	0.09	-0.33	-0.26	0.10	-0.37	0.24	-0.09
CAOV	0.19	-0.10	-0.33	-0.01	0.07	-0.23	-0.16	0.24	0.28	0.22	0.11	0.14
QURU	-0.22	-0.20	-0.25	-0.13	0.21	-0.11	-0.17	-0.07	0.13	0.17	0.12	-0.12
Palmer Drought Severity Index	Apr	May	Jun	Jul	Aug	Sep	Apr	May	Jun	Jul	Aug	Sep
ACSA	-0.05	-0.03	-0.16	-0.21	-0.03	0.01	-0.23	-0.12	-0.03	-0.11	0.07	0.02
CAOV	-0.35	-0.29	-0.33	-0.34	-0.34	-0.32	-0.26	-0.18	0.08	0.19	0.27	0.24
QURU	-0.18	-0.17	-0.25	-0.26	-0.10	-0.12	-0.37	-0.36	-0.18	-0.04	-0.02	-0.07

Literature Cited

Abrams, M. 1998. The red maple paradox. BioScience 48: 355-364.

Adams, H.D., M. Guardiola-Claramonte, G.A. Barron-Gafford, J.C. Villegas, D.D. Breshears, C.B. Zou, P.A. Troch, and T.E. Huxman. 2009. Temperature sensitivity of drought-induced tree mortality portends increased regional die-off under global-change-type drought. Proceedings of the National Academy of Sciences of the United States of America 106:7063-7066.

Albrecht, J. C. 1974. Alterations in the hydrologic cycle induced by urbanization in northern New Castle County, Delaware: magnitudes and projections. U.S. Environmental Protection Agency Library Report Number DI-14-31-0001-3508; DI-14-31-0001-3808; OWRR-A-017-DEL; W74-07729; OWRR-A-017-DEL(2)

Bouyoucos, G.J. 1962. Hydrometer method improved for making particle size analyses of soils. Agronomy Journal. 54(5):464-5.

Clark, J.S. 2005. Why environmental scientists are becoming Bayesians. Ecology Letters 8:2-14.

Churchill, D.J., A.J. Larson, M.C. Dahlgreen, J.F. Franklin, P.F. Hessburg, and J.A. Lutz. 2013. Restoring forest resilience: from reference spatial patterns to silvicultural prescriptions and monitoring. Forest Ecology and Management 291:442-457.

Coomes, D.A., D.F.R.P. Burslem and W.D. Simonson. 2014. Forests and Global Change. Cambridge University Press, Cambridge, UK.

Cowden, M.M., J.L. Hart, and M.L. Buchanan. 2014. Canopy accession strategies and climate response for three Carya species common in the Eastern Deciduous Forest. Trees, 28:223-235.

Cregg B.M., and M.E. Dix. 2001. Tree moisture stress and insect damage in urban areas in relation to heat island effects. Journal of Arboriculture, 27(1):8-17.

Elliott, K.J., C.F. Miniat, N. Pederson, and S.H. Laseter. 2015. Forest tree growth response to hydroclimate variability in the southern Appalachians. Glob Change Biology, 21: 4627–4641.

ESRI. 2013. ArcGIS Desktop: Release 10.2. Redlands, CA: Environmental Systems Research Institute.

Fahey, R.T., M.B. Bialecki, and D.R. Carter. 2013. Tree Growth and Resilience to Extreme drought across an urban land-use gradient. Arboriculture & Urban Forestry, 39(6): 279-285.

Foster T.E., P.A. Schmalzer, G.A. Fox. 2015. Seasonal climate and its differential impact on growth of co-occurring species. European Journal of Forest Research, 134(3):497-510.

Fry, J., G. Xian, S. Jin, J. Dewitz, C. Homer, L. Yang, C. Barnes, N. Herold, and J. Wickham. 2011. Completion of the 2006 National Land Cover Database for the Conterminous United States. Photogrammetric Engineering & Remote Sensing, 77(9):858-864.

Gavier-Pizarro, G.I., V.C. Radeloff, S.I. Stewart, C.D. Huebner, and N.S. Keuler. 2010. Housing is positively associated with invasive exotic plant species richness in New England, USA. Ecological Applications, 20(7):1913-1925.

Gomez-Aparicio, L.R. Garcia-Valdes, P. Ruiz-Benito, M.A. Zalvala. 2011. Disentangling the relative importance of climate, size and competition on tree growth in Iberian forests: implications for forest management under global change. Global Change Biology, 17: 2400–2414.

Gustafson, E.J., and B.R. Sturtevant. 2013. Modeling Forest Mortality Caused by Drought Stress: Implications for Climate Change. Ecosystems, 16: 60-74.

Haddad, N.M., L.A. Brudving, J. Clobert, K.F. Davies, A. Gonzalez, R.D. Holt, T.E. Lovejoy, J.O. Sexton, M.P. Austin, C.D. Collins, W.M. Cook, E.I. Damschen, R.M. Ewers, B.L. Foster, C.N. Jenkins, A.J. King, W.F. Laurance, D.J. Levey, C.R. Margules, B.A. Melbourne, A.O. Nicholls, J.L. Orrock, D. Song, J.R. Townshend. 2015. Habitat fragmentation and its lasting impact on Earth's ecosystems. Science Advances, 1(2): 1-9.

Homer, C., Dewitz, J., Fry, J., Coan, M., Hossain, N., Larson, C., Herold, N., McKerrow, A., VanDriel, J.N., and Wickham, J. 2007. Completion of the 2001 National Land Cover Database for the Conterminous United States. Photogrammetric Engineering and Remote Sensing, 73(4): 337-341.

Homer, C.G., J.A Dewitz, L. Yang, S. Jin, P. Danielson, G. Xian, J. Coulston, N.D. Herold, J.D. Wickham, and K. Megown. 2015. Completion of the 2011 National Land Cover Database for the conterminous United States-Representing a decade of land cover change information. Photogrammetric Engineering and Remote Sensing, 81(5):345-354.

Jiang, Y.T., P. Fu, and Q.H. Weng. 2015. Assessing the Impacts of Urbanization-Associated Land Use/Cover Change on Land Surface Temperature and Surface Moisture: A Case Study in the Midwestern United States. Remote Sensing 7(4):4880-4898.

Kaye, J.P., R.L. McCulley, and I.C. Burke. 2005. Carbon fluxes, nitrogen cycling, and soil microbial communities in adjacent urban, native and agricultural ecosystems. Global Change Biology, 11(4): 575-587.

Kim, H.H. 1992. Urban Heat-Island. International Journal of Remote Sensing, 13(12):2319-2336.

Klos, R.G., G.G. Wang, W.L. Bauerle, and J.R. Rieck. 2009. Drought impact on forest growth and mortality in the southeast USA: an analysis using Forest Health and Monitoring data. Ecological Applications 19:699–708.

Kunstler, G., Albert, C. H., Courbaud, B., Lavergne, S., Thuiller, W., Vieilledent, G., Zimmermann, N. E. and Coomes, D. A. 2011. Effects of competition on tree radial-growth vary in importance but not in intensity along climatic gradients. Journal of Ecology, 99: 300–312.

Le Blanc D.C., and M.A. Terrell. 2009. Radial growth response of white oak to climate in eastern North America. Canadian Journal of Forest Research, 39:2180–2192.

Lévesque M., L. Walthert, and P. Weber. 2016. Soil nutrients influence growth response of temperate tree species to drought. Journal of Ecology 104:377-387.

Lunn, D., Spiegelhalter, D., Thomas, A., Best, N. 2009. The BUGS project: Evolution, critique and future directions (with discussion). Statistics in Medicine, 28: 3049-3082.

Martin-Benito, D. and Pederson, N. 2015. Convergence in drought stress, but a divergence of climatic drivers across a latitudinal gradient in a temperate broadleaf forest. Journal of. Biogeography, 42: 925–937.

Matlack, G.R. 1993. Microenvironment variation within and among forest edge sites in the eastern United States. Biological Conservation, 66(3): 185-194.

McDonald R.I., Urban D.L. 2004. Forest edges and tree growth rates in the North Carolina Piedmont. Ecology 85:2258-2266.

McDonnell, M. J., S. T. A. Pickett, P. Groffman, P. Bohlen, R. V. Pouyat, W. C. Zipperer, R. W. Permelee, M. M. Carreiro, and K. Medley. 1997. Ecosystem processes along an urban-to-rural gradient. Urban Ecosystems 1: 21-36.

Meinzer, F.C., D.R. Woodruff, D.M. Eissenstat, H.S. Lin, T.S. Adams, and K.A. McCulloh. 2013. Above- and belowground controls on water use by trees of different wood types in an eastern US deciduous forest. Tree Physiology, 33(4): 345-356.

Mérian, P., and F. Lebourgeois. 2011. Size-mediated climate-growth relationships in temperate forests: A multi-species analysis. Forest and Ecology Management, 261:1382-1391.

Michigan Geographic Data Library. 2014. Michigan Digital Elevation Model. https://www.mcgi.state.mi.us/mgdl/?rel=thext&action=thmname&cid=13&cat=Digital+Elevation+Model+%28DEM%29

NCDC. 2015. Subset used: January 1985–December 2014. NOAA/National Climatic Data Center, accessed 14 Feb 2015.

Nehrbass-Ahles, C., Babst, F., Klesse, S., Nötzli, M., Bouriaud, O., Neukom, R., Dobbertin, M. and Frank, D. 2014. The influence of sampling design on tree-ring-based quantification of forest growth. Global Change Biology, 20: 2867–2885.

Nowak, D.J., D.E. Crane, and J.C. Stevens. 2006. Air pollution removal by urban trees and shrubs in the United States. Urban Forestry and Urban Greening, 4(3-4):115-123.

Ogle K, Barber JJ, Barron-Gafford GA, Bentley LP, Young JM, Huxman TE, Loik ME, Tissue DT. 2015. Quantifying ecological memory in plant and ecosystem processes. Ecology letters, 1;18(3):221-35.

Pasho, E., J.J. Camarero, M. de Luis, and S.M. Vicente-Serrano. 2011. Impacts of drought at different time scales on forest growth across a wide climatic gradient in north-eastern Spain. Agricultural and Forest Meteorology, 151: 1800–1811.

Peltier, D. M. P., Fell, M. and Ogle, K. (2016), Legacy effects of drought in the southwestern United States: A multi-species synthesis. Ecological Monographs, 86: 312–326.

Reinmann, A.B. and L.R. Hutyra. 2016. Edge effects enhance carbon uptake and its vulnerability to climate change in temperate broadleaf forests. PNAS, 114:107-112.

Sala, O. E., F. S. Chapin, J. J. Armesto, E. Berlow, J. Bloomfield, R. Dirzo, E. Huber- Sanwald, L. F. Huenneke, R. B. Jackson, A. Kinzig, R. Leemans, D. M. Lodge, H. A. Mooney, M. Oesterheld, N. L. Poff, M. T. Sykes, B. H. Walker, M. Walker, and D. H. Wall. 2000. Global biodiversity scenarios for the year 2100. Science, 287:1770-1774.

Savi, T., S. Bertuzzi, S. Branca, M. Tretiach, and A. Nardini. 2014. Drought-induced xylem cavitation and hydraulic deterioration: risk-factors for urban trees under climate change? New Phytologist, 205(3):1106-1116.

Shea, F., and C.E. Watts. 1939. Dumas method for organic nitrogen. Industrial and Engineering Chemistry, Analytical Edition, 11(6): 333–334.

W. D. Shuster, J. Bonta, H. Thurston, E. Warnemuende, and D. R. Smith. 2005 Impacts of impervious surface on watershed hydrology: A review. Urban Water Journal, 2(4):263-275.

Stokes, M.A., and T.L. Smiley. 1968. An Introduction to Tree-ring Dating. University of Arizona Press, Tucson, AZ.

Suarez M.L., L. Ghermandi, and T. Kitzberger. 2004. Factors predisposing episodic drought-induced tree mortality in Nothofagus-site, climatic sensitivity and growth trends. Journal of Ecology, 92: 954-966.

Tang, G., B. Beckage, and B. Smith. 2012. The potential transient dynamics of forests in New England under historical and projected future climate change. Climatic Change, 114: 357.

US Census Bureau. 2010. State and County QuickFacts: Ann Arbor, MI. United States Census Bureau. http://quickfacts.census.gov/qfd/states/26/2603000.html (Accessed April 29, 2015).

Vicca, S., Luyssaert, S., Peñuelas, J., Campioli, M., Chapin, F. S., Ciais, P., Heinemeyer, A., Högberg, P., Kutsch, W. L., Law, B. E., Malhi, Y., Papale, D., Piao, S. L., Reichstein, M., Schulze, E. D. and Janssens, I. A. 2012. Fertile forests produce biomass more efficiently. Ecology Letters, 15:520-526.

Vogelmann, J.E., S.M. Howard, L. Yang, C. R. Larson, B. K. Wylie, and J. N. Van Driel, 2001. Completion of the 1990's National Land Cover Data Set for the conterminous United States, Photogrammetric Engineering and Remote Sensing, 67:650-662.

Walker, B.H., C.S. Holling, S.R. Carpenter and A.P. Kinzig. 2004. Resilience, adaptability and transformability in socio-ecological systems. Ecology and Society, 9(2):5.

White, P.B., van de Gevel, S.L., Grissino-Mayer, H.D., LaForest, L.B. and Deweese, G.G., 2011. Climatic response of oak species across an environmental gradient in the southern Appalachian Mountains, USA. Tree-Ring Research, 67(1):27-37.

Winkler, J.A., R. Arritt, and S. Pryor. 2012. Climate projections for the Midwest: availability, interpretation and synthesis. In Winkler, J.; Andresen, J.; Hatfield, J.; Bidwell, D.; Brown, D., coordinators. U.S. National Climate Assessment Midwest technical input report. Available at http://glisa.msu.edu/docs/NCA/MTIT_Future.pdf. (Accessed November 24, 2013).

Wyckoff, P.H. and J.S. Clark. 2002. The Relationship between Growth and Mortality for Seven Co-Occurring Tree Species in the Southern Appalachian Mountains. Journal of Ecology, 90(4): 604-615.

Xian, G., Homer, C., Dewitz, J., Fry, J., Hossain, N., and Wickham, J., 2011. The change of impervious surface area between 2001 and 2006 in the conterminous United States. Photogrammetric Engineering and Remote Sensing, 77(8): 758-762.

Xiao, Q., E.G. McPherson, J.R. Simpson, and S.L. Ustin. 1998. Rainfall interception by Sacramento's Urban Forest. Journal of Arboriculture, 24(2):235-244.

Yuan, F and ME Bauer. 2007. Comparison of impervious surface area and normalized difference vegetation index as indicators of surface urban heat island effects in Landsat imagery. Remote Sensing of Environment, 106(3):375-386.

Zhou, W.Q., Y.G. Qian, X.M. Li, W.F. Li, and L.J. Han. 2014. Relationships between land cover and the surface urban heat island: seasonal variability and effects of spatial and thematic resolution of land cover data on predicting land surface temperatures. Landscape Ecology, 29(1):153-167.

Supplemental Information

Figure S1. Goodness of fit (R^2) for predicted vs. observed model results, as described in the text

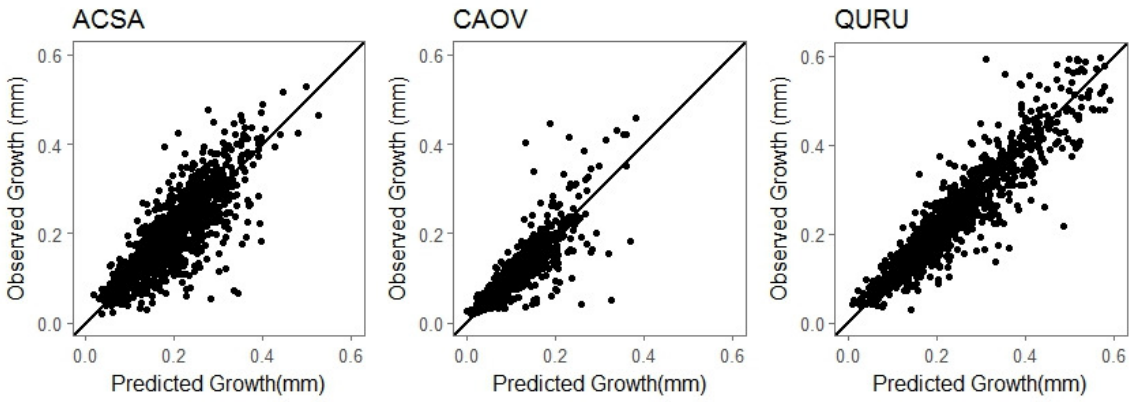

Table S1. Model Parameter Estimates. The model included an intercept (α), percent impervious surface within a 250 m radius (*impervious*) with β as an intercept, antecedent effects of previous growth were estimated as a function of growth with λ as the intercept, ω are the weights given to each year, an individual random effect term (*IRE)* to represent the individual growth variations, a year random effect term (*YRE*) to represent inter-annual variation in growth across all trees. We divided the data, and analyzed accordingly, into three diameter classes, small (<25 cm), medium (25-40 cm), and large (>40 cm). Only small and medium size classes were analyzed for *A. saccharum*.

Species	**Parameter**	**Variable**	**Small Diameter**		**Medium Diameter**		**Large Diameter**	
			Mean±SD	95% CI	Mean±SD	95% CI	Mean±SD	95% CI
ACSA	α	Intercept	0.0584 ± 0.0366	[0.0311,0.0822]	0.0538 ± 0.0252	[0.0296,0.0768]		
	λ	Previous Growth	**0.7638 ± 0.1648**	**[0.6827,0.8707]**	**0.7104 ± 0.1276**	**[0.6180,0.8208]**		
	ω_1	t-1	0.6927 ± 0.1186	[0.4359,0.8947]	0.7272 ± 0.1377	[0.4321,0.9466]		
	ω_2	t-2	0.1407 ± 0.1034	[0.0056,0.3816]	0.1955 ± 0.1292	[0.0090,0.4694]		
	ω_3	t-2	0.1666 ± 0.0935	[0.0155,0.3717]	0.0773 ± 0.0620	[0.0027,0.2309]		
	β	Percent Impervious	**-2.29E-3 ± 1.23E-3**	**[-0.0042,-6.69E-4]**	-2.36E-4 ± 8.57E-4	[-1.83E-3,0.0013]		
CAOV	α	Intercept	0.0085 ± 0.0216	[-0.0021,0.0224]	0.0115 ± 0.0235	[0.0028,0.0219]	0.0103 ± 0.0258	[-0.0017,0.0229]
	λ	Previous Growth	**0.8976 ± 0.0937**	**[0.8017,0.9855]**	**0.8961 ± 0.1243**	**[0.8441,0.9602]**	**0.8915 ± 0.1566**	**[0.8291,0.9726]**
	ω_1	$rw.h_{t-1}$	0.4254 ± 0.1511	[0.0950,0.6694]	0.7605 ± 0.1052	[0.5292,0.9343]	**0**.8812 ± 0.0714	[0.7088,0.9815]
	ω_2	$rw.h_{t-2}$	0.2400 ± 0.1750	[0.0090,0.6158]	0.1728 ± 0.1098	[0.0095,0.4128]	0.0719 ± 0.0647	[0.0021,0.2407]
	ω_3	$rw.h_{t-3}$	0.3347 ± 0.1055	[0.1160,0.5340]	0.0667 ± 0.0495	[0.0027,0.1839]	0.0469 ± 0.0398	[0.0015,0.1472]
	β	Percent Impervious	1.72E-4 ± 3.15E-4	[-2.69E-4,6.29E-4]	-5.21E-5 ± 2.25E-4	[-2.32E-4,1.13E-4]	6.59E-5 ± 2.59E-4	[-1.73E-4,2.91E-4]
QURU	α	Intercept	0.0122 ± 0.0066	[-6.97E-4,0.0254]	0.0112 ± 0.0058	[7.00E-6,0.0228]	0.0140 ± 0.0067	[9.49E-4,0.0272]
	λ	Previous Growth	**0.9606 ± 0.0177**	**[0.9249,0.9945]**	**0.9504 ± 0.0168**	**[0.9157,0.9818]**	**0.9288 ± 0.0210**	**[0.8871,0.9697]**
	ω_1	$rw.h_{t-1}$	0.9176 ± 0.0449	[0.8140,0.9853]	0.7918 ± 0.0643	[0.6540,0.9082]	0.9402 ± 0.0420	[0.8337,0.9927]
	ω_2	$rw.h_{t-2}$	0.0447 ± 0.0396	[0.0013,0.1461]	0.0530 ± 0.0522	[0.0013,0.1924]	0.0435 ± 0.0400	[0.0012,0.1488]
	ω_3	$rw.h_{t-3}$	0.0377 ± 0.0298	[0.0014,0.1106]	0.1553 ± 0.0632	[0.0344,0.2838]	0.0163 ± 0.0155	[4.37E-4,0.0575]
	β	Percent Impervious	5.24E-5 ± 2.10E-4	[-3.60E-4,4.65E-4]	-7.16E-5 ± 2.02E-4	[-4.66E-4,3.25E-4]	8.50E-5 ± 2.87E-4	[-4.78E-4,6.45E-4]

Table S2. Compilation of the basal area (BA, cm^2/m^2) and soil analysis results from the MSU Laboratories.

Forest	Site	BA Average	BA SD	pH	PO_4^-	K^+	Ca^{2+}	Mg^{2+}	Na^+	Cl^-	Total N	Sand	Silt	Clay	Soil Type
Nichols Arboretum	Interior	216.8	44.00	6.2	23	62	1202	168	13	43	0.23	62.2	30.7	7.1	Sandy Loam
Nichols Arboretum	Edge	131.87	55.63	6.5	13	73	1446	247	24	49	0.24	62.1	28.3	9.6	Sandy Loam
Berkshire Creek	Edge	209.8	33.09	6.4	9	90	1557	232	13	41	0.27	60	25.8	14.2	Sandy Loam
Bird Hills	Edge	64		5.6	19	67	1409	220	19	38	0.27	55	30.8	14.2	Sandy Loam
Bird Hills	Interior			5.9	20	47	864	146	9	35	0.1	67.5	19.4	13.1	Sandy Loam
George Reserve	Interior	197.57	78.55	5.3	24	47	416	98	10	38	0.14	83	12.9	4.1	Loamy Sand
Horner McLaughlin	S. Edge	179.57	63.22	5.6	6	70	1041	220	41	41	0.19	51	28.9	20.1	Loam
Horner McLaughlin	N. Edge	210.83	33.27	5.5	10	64	879	185	23	38	0.16	40.3	36.6	23.1	Loam
Horner McLaughlin	Interior	237.5		6.1	7	68	1596	248	20	37	0.22	36.9	36.8	26.3	Loam
North Campus	Edge	230.23	22.50	6.4	23	43	941	129	12	42	0.09	73	17.9	9.1	Sandy Loam
Radrick Forest	Interior	145.47	23.26	5.6	20	50	917	129	13	32	0.15	40	37.6	22.4	Loam
Saginaw Forest	Edge	156.33	61.22	5.8	10	75	1091	178	12	39	0.17	48.2	29.7	22.1	Loam
Scarlett Mitchell	Edge	97.97	33.31	6.1	8	97	1392	263	23	43	0.28	50	29.8	20.2	Loam
Scarlett Mitchell	Interior	143.7	82.56	5.3	16	78	715	138	16	39	0.21	60	24.3	15.7	Sandy Loam
Stapp	Edge	173.87	48.95	6.4	8	75	1414	249	43	36	0.23	49.5	34.3	16.2	Loam
Stinchfield Woods	Interior	132.8	41.99	6.2	33	77	987	169	9	40	0.2	58.5	28.3	13.2	Sandy Loam

Table S3. Model Individual Random Effects (IRE) results by species and tree ID with the standard deviation (SD)

Tree ID	ACSA		CAOV		QURU	
	IRE	SD	IRE	SD	IRE	SD
1	-0.00104	0.007763	-0.00135	0.002944	8.63E-06	0.002352
2	-0.01525	0.009245	-7.14E-04	0.00251	-4.34E-04	0.002467
3	-0.01105	0.008718	0.00162	0.003016	9.06E-04	0.00263
4	0.0113	0.007754	-3.00E-05	0.002795	-9.40E-04	0.002675
5	0.00764	0.007387	-0.0021	0.003131	-2.11E-05	0.002465
6	-0.00351	0.007548	6.81E-04	0.002572	6.26E-04	0.002534
7	-0.00284	0.007324	-5.18E-04	0.002562	-3.10E-04	0.002437
8	-0.00182	0.007532	-1.01E-04	0.002452	-6.36E-04	0.002585
9	-0.0162	0.009069	0.001852	0.003232	-7.45E-04	0.002714
10	-6.93E-04	0.007615	4.08E-04	0.002479	4.40E-04	0.002478
11	-8.21E-04	0.007623	-0.00143	0.002981	-4.75E-04	0.002546
12	-0.01325	0.008308	0.001663	0.003083	-6.78E-04	0.002623
13	-0.00988	0.008235	-2.55E-04	0.002475	0.001154	0.002807
14	-0.00428	0.007607	-4.42E-04	0.002528	3.15E-04	0.002396
15	0.002034	0.007668	4.77E-04	0.002475	-1.17E-04	0.002382
16	0.02208	0.00955	7.02E-04	0.002872	1.37E-04	0.002367
17	-0.01187	0.008409	0.001835	0.002866	-3.40E-04	0.002392
18	0.003911	0.007633	-0.00153	0.00288	7.60E-04	0.002609
19	0.01153	0.008268	-5.29E-04	0.002507	6.68E-04	0.002616
20	0.02084	0.009406	-6.62E-04	0.002529	2.46E-04	0.002444
21	5.89E-04	0.007315	-7.96E-04	0.002565	-3.39E-04	0.002423
22	-3.38E-04	0.007115	1.01E-04	0.002453	-5.43E-04	0.002491
23	0.002276	0.007188	-3.56E-04	0.002463	-3.22E-04	0.002387
24	-0.0064	0.007313	5.01E-04	0.002498	0.001269	0.002988
25	-0.00854	0.007886	-0.00143	0.002753	8.42E-04	0.002668
26	-0.00277	0.007412	8.07E-04	0.002607	-0.00115	0.002919
27	-0.01293	0.008375	-6.30E-04	0.002479	-8.12E-04	0.002631
28	0.001333	0.008802	4.06E-04	0.002512	-3.71E-04	0.002406
29	0.01526	0.009605	-0.00248	0.003845	-9.25E-04	0.002741
30	-0.00746	0.009896	-9.55E-04	0.002563	-3.46E-04	0.002406
31	-0.01182	0.00835	-8.11E-04	0.002662	0.001607	0.003272
32	0.008621	0.00739	0.002382	0.003455	-1.36E-04	0.002391
33	0.002061	0.008091	9.67E-04	0.002518	3.99E-04	0.002551
34	0.01623	0.009031	-3.79E-04	0.002528	-7.51E-04	0.002652
35	0.02379	0.009854	-8.48E-04	0.002595	-5.19E-04	0.00247
36	-0.0075	0.007506	0.0013	0.00276	-7.44E-04	0.002602
37			3.62E-05	0.002558	0.001267	0.003047
38			0.002573	0.003443	7.47E-04	0.002739
39					-4.01E-04	0.002459
40					0.001336	0.002993
41					-3.73E-04	0.002444
42					-2.21E-04	0.002398
43					-1.07E-04	0.002388

Table S4. Values for DBH, distance from roads, percent slope, distance from edge, and percent impervious surface for each tree that was cored. The distances are all measured in meters and were calculated from GIS data extraction through AcrGIS.

Forest	Site	Species	Tree ID	DBH	Distance from Roads	Percent Slope	Distance from Edge	Percent Impervious Surface (250m)		
								2001	2006	2011
ARB	E1	ACSA	1	39.1	60	29.34714	60	9.411167	9.619289	9.619289
ARB	E1	ACSA	2	29.6	67.08204	15.81435	60	10.56853	10.77665	10.77665
ARB	E1	ACSA	3	32.7	60	29.34714	30	10.55838	10.7665	10.7665
BDHS	E	ACSA	4	29.3	30	81.60002	60	1.57868	1.57868	1.57868
BDHS	E	ACSA	5	24.6	30	81.60002	60	1.57868	1.57868	1.57868
BDHS	E	ACSA	6	17.2	60	71.4826	67.08204	1.573604	1.573604	1.573604
BDHS	I	ACSA	7	39.7	212.132	4.064018	182.4829	0.80203	0.80203	0.80203
BDHS	I	ACSA	8	32.3	212.132	40.84909	210	0.274112	0.274112	0.274112
BDHS	I	ACSA	9	26.4	228.4732	32.6747	228.4732	0.025381	0.025381	0.025381
GR	I	ACSA	10	19.6	500	5	256.32	0	0	0
GR	I	ACSA	11	18.6	500	7	305.94	0	0	0
GR	I	ACSA	12	18.7	500	10	305.94	0	0	0
HM	E1	ACSA	13	14.9	94.86833	16.53136	84.85281	0.203046	0.203046	0.203046
HM	E1	ACSA	14	20.8	67.08204	21.75566	42.42641	0.228426	0.228426	0.228426
HM	E1	ACSA	15	18	90	20.83468	67.08204	0.203046	0.203046	0.203046
HM	E2	ACSA	16	27.1	150	0	108.1665	7.502538	7.502538	7.502538
HM	E2	ACSA	17	19.9	150	0	108.1665	7.502538	7.502538	7.502538
HM	E2	ACSA	18	35.1	90	18.7154	60	8.761421	8.761421	8.761421
HM	I	ACSA	19	21.1	150	14.40457	134.1641	0.746193	0.746193	0.746193
HM	I	ACSA	20	26.3	152.9706	16.77581	161.5549	2.786802	2.786802	2.786802
HM	I	ACSA	21	22	152.9706	16.77581	134.1641	0.746193	0.746193	0.746193
NC	E	ACSA	22	28.7	271.6616	44.68246	30	2.878173	2.918782	2.928934
NC	E	ACSA	23	37	270	47.18373	30	3.228426	3.228426	3.228426
NC	E	ACSA	24	23.4	240	29.05635	0	3.852792	3.852792	3.857868
RAD	I	ACSA	25	31.1	330	15.49302	108.1665	0.365482	0.365482	0.365482
RAD	I	ACSA	26	45.2	330	15.49302	108.1665	0.329949	0.329949	0.329949
RAD	I	ACSA	27	29	330	17.66953	108.1665	0.365482	0.365482	0.365482
SAG	E	ACSA	28	22.3	228.4732	10.90842	0	15.48731	15.48731	15.71574
SAG	E	ACSA	29	38.6	241.8677	20.44072	0	12.533	12.533	12.76142
SAG	E	ACSA	30	14.8	201.2461	21.52538	0	15.48731	15.48731	15.71574
SM	I	ACSA	31	13.1	271.6616	8.7509	150	4.720812	4.720812	4.720812
SM	I	ACSA	32	25.1	301.4963	6.318217	150	4.624365	4.624365	4.624365
SM	I	ACSA	33	15.4	300	0.457563	90	10.29442	10.29442	10.50761
SW	I	ACSA	34	38.2	780.5767	4.970695	108.1665	0	0	0
SW	I	ACSA	35	38	780.5767	4.970695	108.1665	0	0	0
SW	I	ACSA	36	24.2	768.3749	6.912838	123.6932	0	0	0
ARB	E1	CAOV	1	24	67.08204	43.29435	42.42641	4.639594	4.847716	4.847716
ARB	E1	CAOV	2	31.3	67.08204	43.29435	42.42641	4.639594	4.847716	4.847716
ARB	E1	CAOV	3	48.9	84.85281	60.31552	67.08204	4.624365	4.832487	4.832487
ARB	E2	CAOV	4	24.9	60	47.78124	30	27.51269	27.51269	28
ARB	E2	CAOV	5	38.7	42.42641	29.20827	30	26.71066	26.71066	27.19797
ARB	E2	CAOV	6	40.4	30	24.97906	0	34.58883	34.58883	35.07614
BC	E	CAOV	7	49.5	108.1665	19.77522	0	25.40101	30.42132	30.62944
BC	E	CAOV	8	42.1	42.42641	12.58633	0	26.1066	30.88833	31.09645

BC	E	CAOV	9	30.4	67.08204	28.37932	0	24.11675	28.88325	29.09137
BDHS	E	CAOV	10	41.4	30	89.34985	30	1.335025	1.335025	1.335025
BDHS	E	CAOV	11	58	30	89.34985	30	1.335025	1.335025	1.335025
BDHS	E	CAOV	12	26.1	30	81.60002	60	1.57868	1.57868	1.57868
HM	E1	CAOV	13	43.5	94.86833	16.53136	84.85281	0.203046	0.203046	0.203046
HM	E1	CAOV	14	31.8	67.08204	15.0332	67.08204	0.228426	0.228426	0.228426
HM	E1	CAOV	15	36.8	30	17.25757	67.08204	0.228426	0.228426	0.228426
HM	E2	CAOV	16	42.5	108.1665	4.529297	0	73.78172	73.78172	73.78172
HM	E2	CAOV	17	42.9	90	7.886551	60	8.543147	8.543147	8.543147
HM	E2	CAOV	18	29.3	150	0	108.1665	7.502538	7.502538	7.502538
HM	I	CAOV	19	43.5	152.9706	16.77581	134.1641	0.746193	0.746193	0.746193
HM	I	CAOV	20	37.4	152.9706	16.77581	150	0.939086	0.939086	0.939086
HM	I	CAOV	21	29.7	134.1641	18.96575	127.2792	0.213198	0.213198	0.213198
NC	E	CAOV	22	37.2	240	35.97911	67.08204	3.203046	3.238579	3.238579
RAD	I	CAOV	23	28.6	330	15.49302	108.1665	0.365482	0.365482	0.365482
RAD	I	CAOV	24	33.2	330	15.49302	84.85281	0.446701	0.446701	0.446701
RAD	I	CAOV	25	44.6	330	14.03501	84.85281	0.446701	0.446701	0.446701
SAG	E	CAOV	26	42.5	308.8689	14.70132	30	6.57868	6.57868	6.807106
SAG	E	CAOV	27	22.2	295.4657	14.67252	30	6.57868	6.57868	6.807106
SAG	E	CAOV	28	37.3	295.4657	14.67252	30	6.57868	6.57868	6.807106
SM	E	CAOV	29	48.1	120	4.404655	42.42641	14.16751	14.16751	14.38071
SM	E	CAOV	30	23.6	120	5.286943	30	16.06091	16.06091	16.27411
SM	E	CAOV	31	38	120	5.286943	30	16.06091	16.06091	16.27411
SM	I	CAOV	32	23	268.3282	11.02255	180	2.081218	2.081218	2.081218
SM	I	CAOV	33	45.8	271.6616	8.7509	180	1.964467	1.964467	1.964467
SM	I	CAOV	34	28.2	256.3201	7.827662	180	2.111675	2.314721	2.314721
STP	E	CAOV	35	50.5	30	18.19589	30	23.92386	23.92386	24.54315
STP	E	CAOV	36	30.4	30	18.19589	42.42641	23.04061	23.04061	23.6599
STP	E	CAOV	37	32.9	84.85281	10.63823	67.08204	22.08629	22.08629	22.70558
SW	I	CAOV	38	21.6	810	8.476509	60	0	0	0
SW	I	CAOV	39	24.9	840	7.950051	42.42641	0	0	0
SW	I	CAOV	40	40	780	8.195452	30	0	0	0
ARB	E1	QURU	1	51.7	67.08204	58.26918	42.42641	7.055838	7.263959	7.263959
ARB	E1	QURU	2	35.9	94.86833	53.09673	42.42641	7.106599	7.314721	7.314721
ARB	E1	QURU	3	42.7	108.1665	57.25875	60	8.243655	8.451777	8.451777
ARB	E2	QURU	4	25.8	30	75.40462	30	22.42132	22.42132	22.90863
ARB	E2	QURU	5	42.7	30	106.7394	30	27.57361	27.57361	28.06091
ARB	E2	QURU	6	22.2	42.42641	73.61371	42.42641	21.68528	21.68528	22.17259
BC	E	QURU	7	30	108.1665	19.77522	0	25.40101	30.42132	30.62944
BC	E	QURU	8	42.3	84.85281	18.00332	0	26.66497	31.68528	31.8934
BC	E	QURU	9	19.3	84.85281	18.00332	0	22.96447	27.49239	27.70051
BDHS	E	QURU	10	59.5	60	71.4826	67.08204	1.573604	1.573604	1.573604
BDHS	E	QURU	11	16.5	30	89.34985	30	1.335025	1.335025	1.335025
BDHS	E	QURU	12	27.9	90	51.31572	90	0.690355	0.690355	0.690355
BDHS	I	QURU	13	55.6	218.4033	39.95954	212.132	0.152284	0.152284	0.152284
BDHS	I	QURU	14	36.5	218.4033	39.95954	218.4033	0.091371	0.091371	0.091371
BDHS	I	QURU	15	31.2	218.4033	39.95954	218.4033	0.091371	0.091371	0.091371
GR	I	QURU	16	49.1	500	7	276.586	0	0	0
GR	I	QURU	17	45.4	500	7	313.209	0	0	0
GR	I	QURU	18	29.5	500	7	256.32	0	0	0
HM	E1	QURU	19	37.9	67.08204	21.75566	42.42641	0.228426	0.228426	0.228426

HM	E1	QURU	20	41	30	17.25757	42.42641	0.228426	0.228426	0.228426
HM	E1	QURU	21	26.4	60	19.89071	42.42641	0.228426	0.228426	0.228426
HM	E2	QURU	22	48.2	60	8.865218	30	9.375634	9.375634	9.375634
HM	E2	QURU	23	26.2	60	15.01146	0	9.517767	9.517767	9.517767
HM	E2	QURU	24	28.3	60	8.677253	30	9.177665	9.177665	9.177665
NC	E	QURU	25	43.4	276.5863	47.3511	0	2.908629	2.918782	2.918782
NC	E	QURU	26	33.9	270	45.74439	60	2.847716	2.857868	2.857868
NC	E	QURU	27	23.7	270	40.71983	30	2.796954	2.796954	2.796954
RAD	I	QURU	28	53.1	330	17.66953	127.2792	0.233503	0.233503	0.233503
RAD	I	QURU	29	35.6	300	13.07476	84.85281	0.446701	0.446701	0.446701
RAD	I	QURU	30	50.2	390	15.25938	127.2792	0.071066	0.071066	0.071066
SAG	E	QURU	31	38.2	366.1967	32.73742	30	4.781726	4.781726	4.781726
SAG	E	QURU	32	25.6	161.5549	21.94633	30	19.16244	19.16244	20.02538
SAG	E	QURU	33	30.9	212.132	9.702703	30	18.38071	18.38071	18.60914
SM	E	QURU	34	19.7	120	5.286943	42.42641	19.50254	19.50254	19.71574
SM	E	QURU	35	53.4	120	3.410397	30	21	21	21.2132
SM	E	QURU	36	21.2	120	5.286943	30	16.06091	16.06091	16.27411
SM	I	QURU	37	28.8	268.3282	11.02255	180	2.081218	2.081218	2.081218
SM	I	QURU	38	61	271.6616	8.7509	150	4.624365	4.624365	4.624365
SM	I	QURU	39	42.4	268.3282	11.02255	150	4.720812	4.720812	4.720812
STP	E	QURU	40	36.6	42.42641	18.81428	30	25.6599	25.6599	26.27919
STP	E	QURU	41	21.2	42.42641	18.81428	60	25.3198	25.3198	25.93909
STP	E	QURU	42	30.1	42.42641	18.81428	60	25.3198	25.3198	25.93909
SW	I	QURU	43	51.2	782.3043	8.566132	108.1665	0	0	0
SW	I	QURU	44	57.1	725.6032	5.559006	174.9286	0	0	0
SW	I	QURU	45	33.5	807.7747	8.175746	123.6932	0	0	0

S5. Open BUGS Code used to run models for each species: ACSA, CAOV, and QURU

ACSA model{

```
for(i in 1:36) {                                                    #number of trees
   for(t in 1:3){   rw.h[i,t]~dnorm(rwl[i,t], tau[1])C(0,)}  #prediction, first 3 years
   for(t in 4:30){                                          # number of years modeled, 1988 to 2014
         rwl[i,t]~dnorm(G[i,t], tau[1])                          #likelihood
         rw.h[i,t]~dnorm(G[i,t], tau[1])                  #prediction

#process model
G[i,t] <- alpha[1]*st1[i,t]+alpha[2]*st2[i,t]+lam[1]*st1[i,t]*(w[1]*rw.h[i,t-1]+w[2]*rw.h[i,t-2]+w[3]*rw.h[i,t-
3])+lam[2]*st2[i,t]*(v[1]*rw.h[i,t-1]+v[2]*rw.h[i,t-2]+v[3]*rw.h[i,t-
3])+beta[1]*st1[i,t]*imp[i]+beta[2]*st2[i,t]*imp[i]+IRE[i]+YRE[t]

}}

# Priors
    w[1:3]~ddirich(wm[])
    v[1:3]~ddirich(vm[])
for(k in 1:3){
   wm[k]<-1
   vm[k]<-1
}

for(i in 1:2){
    alpha[i]~dnorm(0,0.0001)
}

for(i in 1:2){
    lam[i]~dnorm(0,0.0001)
}

for(i in 1:2){
    beta[i]~dnorm(0,0.0001)
}

for(i in 1:36){ IRE[i]~dnorm(0, tau[2])} #36 is the number of trees
for(i in 4:30){YRE[i]~dnorm(0, tau[3])} #30 is the number of years

    for(i in 1:3){
        tau[i]<-1/(sigma[i]*sigma[i])
        sigma[i]~dunif(0,100)
        }

#simulated predictions
#at a diameter of 15.58 for small and 31.03 (based on the data, averages)
#growth the previous 3 years was average, for small diameter 0.1733, for large diameter 0.2183

ire~dnorm(0,tau[2])
yre~dnorm(0,tau[3])

for(i in 1:8){

#small diameter
```

```
Gp[1,i] <- alpha[1]+lam[1]*0.1733+beta[1]*impP[i]+ire+yre
rwP[1,i]~dnorm(Gp[1,i], tau[1])C(0,) #prediction

#large diameter
Gp[2,i] <- alpha[2]+lam[2]*0.2183+beta[2]*impP[i]+ire+yre
rwP[2,i]~dnorm(Gp[2,i], tau[1])C(0,) #prediction
}

}
```

Model

```
#initials
list(sigma=c(1,1,1),  alpha = c(0.1,0.1), lam = c(0,0), beta= c(0,0) )
#data simulations
list(impP = c(0,5,10,15,20,25,30,35))
```

CAOV model {

```
for(i in 1:38) {                                              #number of trees
    for(t in 1:3){ rw.h[i,t]~dnorm(rwl[i,t], tau[1])C(0,)} #prediction,  first 3 years
    for(t in 4:30){                                          # number of years modeled, 1988 to 2014
          rwl[i,t]~dnorm(G[i,t], tau[1])                       #likelihood
          rw.h[i,t]~dnorm(G[i,t], tau[1])                      #prediction

#process model
G[i,t] <- alpha[1]*st1[i,t]+alpha[2]*st2[i,t]+alpha[3]*st3[i,t]+gg2[i,t]+gg3[i,t]

    gg2[i,t]<-lam[1]*st1[i,t]*(w[1]*rw.h[i,t-1]+w[2]*rw.h[i,t-2]+w[3]*rw.h[i,t-    3])+lam[2]*st2[i,t]*(v[1]*rw.h[i,t-
    1]+v[2]*rw.h[i,t-2]+v[3]*rw.h[i,t-3])+lam[3]*st3[i,t]*(u[1]*rw.h[i,t-1]+u[2]*rw.h[i,t-2]+u[3]*rw.h[i,t-3])

    gg3[i,t]<-beta[1]*st1[i,t]*imp[i]+beta[2]*st2[i,t]*imp[i]+beta[3]*st3[i,t]*imp[i]+IRE[i]+YRE[t]

}}

# Priors
    w[1:3]~ddirich(wm[])
    v[1:3]~ddirich(vm[])
    u[1:3]~ddirich(um[])
for(k in 1:3){
    wm[k]<-1
    vm[k]<-1
    um[k]<-1
}
    for(i in 1:3){
    alpha[i]~dnorm(0,0.0001)
          }
    for(i in 1:3){
    lam[i]~dnorm(0,0.0001)
          }
    for(i in 1:3){
```

```
    beta[i]~dnorm(0,0.0001)
        }

for(i in 1:38){ IRE[i]~dnorm(0, tau[2])} #38 is the number of trees
for(i in 4:30){YRE[i]~dnorm(0, tau[3])} #30 is the number of years

    for(i in 1:3){
        tau[i]<-1/(sigma[i]*sigma[i])
        sigma[i]~dunif(0,100)
        }

#simulated predictions

#growth the previous 3 years was average, for small diameter 0.0996, for medium diameter 0.1008, large
diameter 0.1267

ire~dnorm(0,tau[2])
yre~dnorm(0,tau[3])

for(i in 1:8){

#small diameter
Gp[1,i] <- alpha[1]+lam[1]*0.0996+beta[1]*impP[i]+ire+yre
rwP[1,i]~dnorm(Gp[1,i], tau[1])C(0,) #prediction

#medium diameter
Gp[2,i] <- alpha[2]+lam[2]*0.1008+beta[2]*impP[i]+ire+yre
rwP[2,i]~dnorm(Gp[2,i], tau[1])C(0,) #prediction

#large diameter
Gp[3,i] <- alpha[3]+lam[3]*0.1267+beta[3]*impP[i]+ire+yre
rwP[3,i]~dnorm(Gp[3,i], tau[1])C(0,) #prediction

}

}
```

Model

```
#initials
list(sigma=c(1,1,1),  alpha = c(0.1,0.1,0.1), lam = c(0,0,0), beta=c(0,0,0) )

#data simulations
list(impP = c(0,5,10,15,20,25,30,35))
```

QURU model {

```
for(i in 1:43) {                                          #number of trees
    for(t in 1:3){ rw.h[i,t]~dnorm(rwl[i,t], tau[1])C(0,)} #prediction,  first 3 years
    for(t in 4:30){                                      # number of years modeled, 1988 to 2014
          rwl[i,t]~dnorm(G[i,t], tau[1])                   #likelihood
          rw.h[i,t]~dnorm(G[i,t], tau[1])                  #prediction

#process model
G[i,t] <- alpha[1]*st1[i,t]+alpha[2]*st2[i,t]+alpha[3]*st3[i,t]+gg2[i,t]+gg3[i,t]

    gg2[i,t]<-lam[1]*st1[i,t]*(w[1]*rw.h[i,t-1]+w[2]*rw.h[i,t-2]+w[3]*rw.h[i,t-    3])+lam[2]*st2[i,t]*(v[1]*rw.h[i,t-
    1]+v[2]*rw.h[i,t-2]+v[3]*rw.h[i,t-3])+lam[3]*st3[i,t]*(u[1]*rw.h[i,t-1]+u[2]*rw.h[i,t-2]+u[3]*rw.h[i,t-3])

    gg3[i,t]<- beta[1]*st1[i,t]*imp[i]+beta[2]*st2[i,t]*imp[i]+beta[3]*st3[i,t]*imp[i]+IRE[i]+YRE[t]
}}

# Priors
    w[1:3]~ddirich(wm[])
    v[1:3]~ddirich(vm[])
    u[1:3]~ddirich(um[])
for(k in 1:3){
    wm[k]<-1
    vm[k]<-1
    um[k]<-1
}
    for(i in 1:3){
    alpha[i]~dnorm(0,0.0001)
          }
    for(i in 1:3){
    lam[i]~dnorm(0,0.0001)
          }
    for(i in 1:3){
    beta[i]~dnorm(0,0.0001)
          }

for(i in 1:38){ IRE[i]~dnorm(0, tau[2])} #38 is the number of trees
for(i in 4:30){YRE[i]~dnorm(0, tau[3])} #30 is the number of years

    for(i in 1:3){
          tau[i]<-1/(sigma[i]*sigma[i])
          sigma[i]~dunif(0,100)
          }

#simulated predictions

#at a diameter of 17.03 for small, 31.90 for medium and 47.62 (based on the data, averages)
#growth the previous 3 years was average, for small diameter 0.2378, for medium diameter 0.2083, large
diameter 0.2099
```

```
ire~dnorm(0,tau[2])
yre~dnorm(0,tau[3])

for(i in 1:8){

#small diameter
Gp[1,i] <- alpha[1]+lam[1]*0.2378+beta[1]*impP[i]+ire+yre
rwP[1,i]~dnorm(Gp[1,i], tau[1])C(0,) #prediction

#medium diameter
Gp[2,i] <- alpha[2]+lam[2]*0.2083+beta[2]*impP[i]+ire+yre
rwP[2,i]~dnorm(Gp[2,i], tau[1])C(0,) #prediction

#large diameter
Gp[3,i] <- alpha[3]+lam[3]*0.2099+beta[3]*impP[i]+ire+yre
rwP[3,i]~dnorm(Gp[3,i], tau[1])C(0,) #prediction
}

}
```

Model

```
#initials
list(sigma=c(1,1,1),  alpha = c(0.1,0.1,0.1), lam = c(0,0,0) beta = c(0,0,0) )

#data simulations
list(impP = c(0,5,10,15,20,25,30,35))
```